Environmental Science Nano

PAPER

Cite this: *Environ. Sci.: Nano*, 2016, 3, 1027

Determination of inequable fate and toxicity of Ag nanoparticles in a *Phanerochaete chrysosporium* biofilm system through different sulfide sources†

Zhi Guo,[ab] Guiqiu Chen,*[ab] Guangming Zeng,*[ab] Jie Liang,[ab] Binbin Huang,[ab] Zhihua Xiao,[c] Feng Yi,[ab] Zhenzhen Huang[ab] and Kai He[ab]

Received 2nd June 2016,
Accepted 8th July 2016

DOI: 10.1039/c6en00156d

rsc.li/es-nano

Nanomaterials, especially silver nanoparticles (AgNP), are widely used in consumer products, yet their environmental fate and risk to biological wastewater treatment systems is poorly understood. In this study, we investigated the distribution of AgNP coated with polyvinylpyrrolidone (PVP) and citrate (Cit) (PVP-AgNP and Cit-AgNP, respectively) in a *Phanerochaete chrysosporium* (*P. chrysosporium*) biofilm microcosm, with either the organic sulfide, cysteine, or the inorganic sulfide, Na_2S, present in the test environment. Both types of AgNP tested easily penetrated the *P. chrysosporium* biofilm and remained mostly in the bottom layer (1.6–2.0 cm) when cysteine was present. In contrast, both types of AgNP remained in the surface layer (0–0.4 cm) in an aggregated form in the presence of Na_2S. An obvious particle-specific toxicity to the film was observed, despite the inhibited Ag^+ release in cysteine-abundant surroundings. In the presence of Na_2S, the toxicity of both types of AgNP was completely inhibited. In conclusion, this work indicates that sulfide-induced particle stability (cysteine has no effect on Cit-AgNP and induced a smaller size of PVP-AgNP, and Na_2S caused both types of AgNP to aggregate) was crucial to AgNP transfer and toxicity in biofilms.

Nano impact

This study illustrates the specific transfer of AgNP into each biofilm layer and the final removal efficiency in the presence of cysteine or Na_2S. It provides useful information to those using biofilms in the wastewater treatment field. The loss of bioavailable free silver as a result of sulfidation decreased the overall acute biofilm toxicity, but different sulfide sources had inequable influence on the toxicity of AgNP to biofilms. Environmental sulfide may simultaneously affect the activity of biofilm cells, in turn, producing distinguished processing capacity of wastewater. Compared to previous works, this study has made the following progress: (1) determined the inequable fate and toxicity of AgNP induced by different sulfide sources; (2) a *Phanerochaete chrysosporium* biofilm was used as the test system; and (3) studied the specific distribution in different biofilm layer depths in detail.

1. Introduction

The wide use of silver nanoparticles (AgNP) in consumer and health care products makes their release to waste streams and the environment inevitable. This has raised great concern about the environmental safety of AgNP.[1,2] Once AgNP enter aquatic environments, many factors (*e.g.*, pH, ionic strength, and ligands present) may cause profound physical and chemical changes, which greatly impact the fate, transport, and toxicity of AgNP.[3–5] The insufficient knowledge of the fate of AgNP in natural waters has made it challenging for biological wastewater treatment systems in terms of these emerging contaminants.[6]

The environmental impact of AgNP is caused mostly by their mobility and aggregation behavior in natural and engineered environments. These actions are governed by the

[a] *College of Environmental Science and Engineering, Hunan University, Changsha 410082, PR China. E-mail: gqchen@hnu.edu.cn, zgming@hnu.edu.cn; Fax: +86 731 88823701; Tel: +86 731 88822829*
[b] *Key Laboratory of Environmental Biology and Pollution Control (Hunan University), Ministry of Education, Changsha 410082, PR. China*
[c] *College of Bioscience and Biotechnology, Hunan Agricultural University, Changsha, Hunan, 410128, China*

† Electronic supplementary information (ESI) available: Figures showing TEM, LSPR absorbance of AgNP, photographs of quartz sands and *P. chrysosporium* pellets, zeta potential of AgNP after adding various concentrations of cysteine and Na_2S, dissolved silver concentrations after reaction with sulfide, reservation ratio of quartz sands for AgNP, Cit-AgNP induced viability in the presence of sulfide, effect of sulfide on the toxicity of Ag^+ and intracellular ROS production; tables detailing AgNP stock suspension changes, and relevant parameters of the water sample. See DOI: 10.1039/c6en00156d

physicochemical properties of the particles, including size and surface charge,[7–11] and are directly influenced by the solution conditions.[12,13] Consequently, by evaluating the effects of each environmental factor on the physicochemical properties of the particles under controlled laboratory conditions, specific information on the stability of AgNP can be obtained and predictions for the fate and behavior of the AgNP in various aquatic systems can be made.[14–16] At present, important information on the fate of AgNP used for stability tests in artificial exposure media has been reported.[17–19] Studies on the fate of AgNP in natural freshwater locations are currently needed to validate these results.

Recently, Wirth *et al.*[20] have investigated the effects of exposure to AgNP on the viability of a single bacterial species, *Pseudomonas fluorescens*, *via* dye staining methods. The results indicated that the toxicity of the AgNP was strongly dependent on particle stability, providing a useful metric for the colloidal stability of AgNP that can be used in the prediction of the fate and transport of AgNP in natural and engineered systems. Common ligands that are prevalent in aquatic systems (*e.g.*, Cl^-, S^{2-}, cysteine, and phosphate) may react with AgNP, thus affecting their fate in the ecosystem.[21,22] The reduced sulfur species are considered the most important for the binding of AgNP to form Ag_2S, with a high solubility product equilibrium constant of approximately $10^{-50.1}$.[23] Different capping agents have diverse effects on AgNP surface properties and may present distinguishable dynamic behavior after coming into contact with environmental ligands. To date, no common ligands have been investigated for their effect on special biofilms with AgNP that have been modified with different capping agents. Furthermore, the impact of common ligands on the particle-specific toxicity of AgNP (*i.e.*, Ag^+ release is inhibited) is still not well understood.

As emerging contaminants, AgNP may cause diverse responses from biological wastewater treatment technologies. Hence, it is vital to explore, in depth, the fate and toxicity of AgNP in a specific biological treatment system. *Phanerochaete chrysosporium* (*P. chrysosporium*) has been used extensively in wastewater treatment for its great vitality and strong pollution removal capacity.[24–26] Based on this, the objectives of this work were to determine the fate of AgNP in biofilm systems of the model fungus, *P. chrysosporium* strain BKMF-1767, and determine whether different sulfide sources induce inequable fates. The use of a single-species biofilm microcosm from natural water samples with controlled dosing of the organic sulfide, cysteine, or the inorganic sulfide, Na_2S, represents the biological wastewater treatment system in practical application while preserving variable control and invariant consistency. The dispersion of AgNP coated with polyvinylpyrrolidone (PVP) and citrate (Cit) (PVP-AgNP and Cit-AgNP, respectively) within biofilms, in the presence of the organic sulfide, cysteine, or the inorganic sulfide, Na_2S, was measured to determine their specific distribution within the biofilm layers. Because dissolved silver (Ag^+) release, which is one of the disputed toxicity causes of particle-specific toxicity, will be affected by the sulfide, the particle-specific toxicities of the two types of AgNP were compared. This study shows that both particle stability and Ag^+ were influenced by different sulfide sources, promoting the inequable fate in and toxicity to a *P. chrysosporium* biofilm of AgNP.

2. Experimental section

2.1. Preparation and characterization of AgNP suspensions

Two different coated AgNP, PVP-AgNP and Cit-AgNP, were used in this study. PVP-AgNP was synthesized following the literature[27] with slight modification. Briefly, 70 mL of 1 mM silver nitrate was reduced with 180 mL of 2 mM sodium borohydride (>99% purity, Sigma-Aldrich) in the presence of 0.3% PVP10 (Mw 10 000, Sigma-Aldrich) in an ice bath. After 3 min, the solution was continuously stirred at room temperature for additional 1 h. All particle suspensions were cleaned by a diafiltration method using a 1 kDa regenerated cellulose membrane to remove excess PVP and silver ions. The resulting concentrated AgNP solution (37.62 mg L^{-1}) with an average primary particle diameter of 9.8 ± 6.0 nm based on transmission electron microscopy (TEM, Fig. S1A of the ESI†), was stored at 4 °C in the dark for later use.

Cit-AgNP was synthesized according to the method described by Liu *et al.*[28] A 59.8 mL solution containing 0.6 mM trisodium citrate and 0.4 mM $NaBH_4$ was prepared in double distilled water and stirred vigorously in an ice bath. The solution turned yellow upon the addition of 0.55 mL of 23.5 mM $AgNO_3$, indicating the formation of the AgNP. After 3 h of additional stirring at room temperature, the soluble by-products were removed by diafiltration (molecular weight cut-off of 1000). The TEM images confirmed the spheroidal particles with an average diameter of 7.3 ± 8.3 nm (ESI,† Fig. S1B).

Both of the AgNP have preferable stability in stock solutions (28.77 mg L^{-1} for Cit-AgNP) with negligible size and zeta-potential changes during the experiment in a sealed vessel. The Ag^+ concentrations in the stock solution at 0, 1 month, 3 month, and 5 month were determined by filtering 4 mL of the stock solution through an ultrafiltration centrifuge tube (1 kDa) and measuring the total dissolved silver concentration in the filtrate by ICP-MS (ESI,† Table S1).

2.2. Real water sample collection and pretreatment

The natural water samples (pH 7.22) were collected from Xiangjiang River at 112.95E, 28.18 N. Before use, the water samples were rested for 20 days and then filtered to remove oils and excess organic impurities. The chlorine in the filtrate was eliminated by slightly boiling the samples for 10 min.[29] No obvious interference concentrations of Ag and S^{2-} (Table S2†) were detected in the pretreated samples.

2.3. Strain culture

P. chrysosporium has been selected as the biofilm microbe which has been extensively used for its ability in wastewater decontamination. The *P. chrysosporium* strain BKMF-1767

(ATCC 24725) was obtained from the China Center for Type Culture Collection (Wuhan, China). Stock cultures were maintained on malt extract agar slants at 4 °C. All the additional chemicals include 1.5 g L^{-1} $MgSO_4 \cdot 7H_2O$, 3 g L^{-1} KH_2PO_4, and 20 g L^{-1} glucose as the carbon source. Spores were gently scraped from the agar surface and blended in sterile distilled water to obtain a spore suspension. The spore concentration was adjusted to 2.0×10^6 spores per mL. Aqueous suspensions of fungal spores were inoculated into Kirk's liquid culture medium in 500 mL Erlenmeyer flasks at 37 °C.[30]

2.4. Microcosm design and *Phanerochaete chrysosporium* biofilm growth

To simulate water treatment in a biological filter system, the microcosm was established for 180 × 130 × 150 mm environmental matrices with several dots on the front wall for facilitating sampling (ESI,† Fig. S2). The texture was treated quartz to maximally avoid adsorbing AgNP at its walls. The microcosm was soaked and washed with 3% HNO_3, and then washed with deionized water three times before filtration. Screened white quartz sands with an average size of 3–6 mm were also washed with 3% HNO_3 and deionized water, and then filled the microcosm to 1 cm thickness at the bottom to act as a filter pad. The quartz sands were close to the ball with several corner angles (ESI,† Fig. S3A).

After 3 days of growth in the liquid medium, *P. chrysosporium* pellets (ESI,† Fig. S3B) were harvested and washed with phosphate-buffered saline (PBS) and then with the treated water sample to remove the medium component of the surface. The washed *P. chrysosporium* pellets were tiled onto quartz sands to achieve a ~2 cm thick biofilm. A micropump was employed to extract the water samples for the domestication of the biofilm for 24 h in a waterfall manner. The average hydraulic retention time was maintained at 15–20 min.

2.5. AgNP filtration using the biofilm

AgNP was added in the natural water samples to achieve our assay concentration of 2 mg L^{-1}. Since our goals at this stage were to determine the effects of sulfide on the AgNP fate, sulfide (1.0 mg L^{-1} and 50.0 mg L^{-1}) was mixed uniformly with the AgNP solution before letting it flow through the biofilm to simulate the real surroundings in a water treatment system. Over 30 min of filtration to stabilize the contact environment, filtrates were extracted from each layer of the film (0, 0.2, 0.6, 1.0, 1.4, 1.8, and 2.0 cm) through the reserved holes (the holes were sealed in advance except for the bottom for the effluent).

Because no Ag^+ was detected in the filtrate, the AgNP concentration of the filtrate was determined by nitric acid/hydrogen peroxide digestion.[21] Briefly, 50 μL of the solution was deposited in 10 mL disposable scintillation vials. The filtrate was digested for 24 h in triplicate with the addition of 2 mL of HNO_3 and 1 mL of H_2O_2, followed by filtration through a 0.45 μm filter membrane to get rid of impurities. The resulting filtrate volume was brought to 8.05 mL with 1% nitric acid, and its concentration was then determined by ICP/MS.

We assess the biofilm by layers, which is based on the depth of the film. The definite thickness of the biofilm was defined as one layer, and the whole biofilm was divided into several layers. The reserved AgNP by each layer of the *P. chrysosporium* biofilm was calculated as $(N_{t-1}–N_t)/N_0 \times 100\%$, where N_{t-1} and N_t are the remaining AgNP concentrations of t-1 and t layer filtrates, and N_0 (2 mg L^{-1}) is the initial concentration of the AgNP–natural water sample mixture, respectively. All data were the average of five sampling data conducted in triplicate of each to ensure reproducibility.

2.6. AgNP toxicity to the biofilm

After the filtration, the biofilm of each layer was subjected to toxicity assay (the cell mycelium was obtained from the same depth of the biofilm as the sampling point of water, *i.e.*, 0, 0.2, 0.6, 1.0, 1.4, 1.8, and 2.0 cm. These samples were used to estimate the biofilm viability at the following depths: 0–0.2, 0.2–0.6, 0.6–1.0, 1.0–1.4, 1.4–1.8, and 1.8–2.0 cm. Cell viability assay was conducted according to Luo *et al.*[31] and our previous report.[32] Briefly, 0.2 g of *P. chrysosporium* biofilm cells of each layer were mixed with 1 mL of an MTT solution (5 g L^{-1}) and the mixture was incubated at 50 °C. The reaction was stopped by adding 0.5 ml of hydrochloric acid (1 M) to the mixture. The mixture was centrifuged (10 000 × g, 5 min), the supernatant was discarded, and the pellets were agitated in 6 ml of propan-2-ol for 2 h at 25 °C. The centrifugation process was repeated and the absorbance of the supernatant was recorded at 534 nm.

Intracellular ROS generation was assessed by monitoring the enhancement of the fluorescence intensity of the exposed samples relative to that of the control, as previously described.[33] *P. chrysosporium* cells were incubated with a nonfluorescent dye, 2,7-dichlorodihydrofluorescein diacetate (H_2DCF-DA, 5 μM), in the incubation medium for 2 h before filtering the AgNP solution in the dark. The biofilm cells were then harvested and washed with PBS, and the fluorescence intensity of the cell extraction filters was measured using a fluorescence spectrometer (FluoroMax-4; Horiba Scientific, Tokyo, Japan) at excitation and emission wavelengths of 485 nm and 525 nm, respectively. H_2DCF-DA could be transformed into the nonfluorescent 2,7-dichlorodihydrofluorescein (H_2DCF) by intracellular esterase if it enters the cells. In the presence of ROS, H_2DCF could be oxidized to the fluorescent 2,7-dichlorofluorescein (DCF). Therefore, an enhanced fluorescence signal produced from DCF is indicative of an elevated level of ROS in the cell.

2.7. Statistical analysis

Statistical analysis was performed on each of the assays. The tests were run three times each and each sample was analyzed in triplicate. A one-way analysis of variance (one-

way ANOVA) was performed with all of the samples, and p-values < 0.05 were considered to be significantly different.

3. Results and discussion

3.1. Particle characterization and stability

The average sizes of AgNP determined by dynamic light scattering (DLS) are included in Fig. 1. The suspensions of AgNP in pure water (deionized water, 18.25 MΩ cm, and the resulting "pure water" was also identical to "deionized water") showed an average hydrodynamic diameter distribution of 39.8 ± 4.3 nm for PVP-AgNP and 24.5 ± 2.7 nm for Cit-AgNP. The different size distributions obtained from transmission electron microscopy (TEM) and DLS resulted from the different measurement principles of the two technologies.[34] The average sizes of the PVP-AgNP and Cit-AgNP in the treated natural water were 40.3 ± 2.8 nm and 25.2 ± 2.1 nm, respectively. No obvious size change was observed in natural water, indicating that both types of AgNP maintained their stability when transferred from pure water to natural water.

Other evidence for the stability of AgNP in natural water is provided by the UV–vis absorbance spectra (ESI,† Fig. S4). These display the expected localized surface plasmon resonance (LSPR) absorbance peaks at 401 nm and 394 nm for PVP-AgNP and Cit-AgNP, respectively, when initially dispersed in pure water, and the peak positions were unaltered after dispersal in natural water. After 2 h in natural water, the solution exhibited a negligible decrease in LSPR absorbance strength of approximately 0.30% for PVP-AgNP and 1.24% for Cit-AgNP. Thus, the natural water did not mask the LSPR absorbance and surface properties of AgNP.[35]

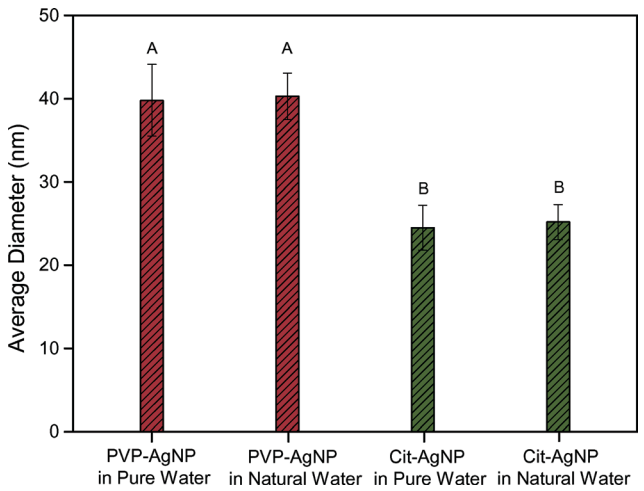

Fig. 1 Size distribution of PVP-AgNP and Cit-AgNP in pure water and natural water. The concentrations of both AgNP were 2 mg L^{-1} in a consistent volume of 4 mL of the water sample. Bars with the same letter represent that the two are not significantly different ($p > 0.05$).

3.2. Sulfide effect on stability and dissolution of AgNP

The effect of the organic sulfide, cysteine, and the inorganic sulfide, Na_2S, on the stability of AgNP was determined using DLS, as shown in Fig. 2. Cysteine did not affect the average size of AgNP, except for a slight decrease in the size of the PVP-AgNP (Fig. 2A). When the concentration of cysteine increased to 100 mg L^{-1}, the average size of the PVP-AgNP decreased by 37.84% compared to the initial average size, whereas a negligible increase of approximately 3.71% was measured in the size of the Cit-AgNP. By comparison, Na_2S induced an average size increase in both PVP-AgNP (Fig. 2A) and Cit-AgNP (Fig. 2B). The average increases were 128.99% for PVP-AgNP and 239.38% for Cit-AgNP in the presence of 100 mg L^{-1} Na_2S. Linear fitting was performed between the size of the AgNP and Na_2S concentration. The size of both types of AgNP correlated well with the Na_2S concentration, as seen in the following linear relationships.

$$y = 34.33 + 6.48x \quad r^2 = 0.99 \text{ for PVP-AgNP}$$
$$y = 20.85 + 7.85x \quad r^2 = 0.97 \text{ for Cit-AgNP}$$

Therefore, cysteine and Na_2S elicited entirely different behaviors from AgNP in water samples. Cysteine maintained and even enhanced the stability of the tested AgNP. However, the linear rise in average size that occurred with increasing Na_2S concentration suggests potential agglomeration of PVP-AgNP and Cit-AgNP at greater Na_2S concentrations.[35] Fig. S5A and B in the ESI† exhibit the ζ potentials of PVP-AgNP and Cit-AgNP after addition of various sulfide sources. Na_2S addition induced lower ζ potentials in comparison with cysteine and may account for the significant size changes in both types of AgNP.

Sulfide at different concentrations apparently resulted in size variation in AgNP, which is consistent with the changes in LSPR absorbance (Fig. 3). Interestingly, a slight blue shift (shift to the left) of the LSPR peaks was observed for the cysteine-treated PVP-AgNP (Fig. 3A), indicating that the smaller size of the particles corresponds to the DLS measurements in Fig. 2A. This can be attributed to surface modification of PVP-AgNP with increasing cysteine concentrations.[36,37] Regarding treatment with Na_2S, both types of AgNP showed a red shift (shift to the right), indicating a significantly larger aggregated size with increasing Na_2S. Sulfide (both cysteine and Na_2S) could significantly mask the LSPR absorbance of the AgNP (including PVP-AgNP and Cit-AgNP) in a concentration-dependent manner. Furthermore, the relatively lower LSPR absorbance of AgNP at higher sulfide concentrations is suggestive of adequate reaction of sulfide with the surface of the AgNP as reported by Liu *et al.*,[37] which can account for the size changes.

The Ag^+ concentrations in the filtrate from ultrafiltration centrifugation after 2 h are shown in Fig. S6 of the ESI.† Ag^+ was approximately 22.92 and 251.12 times more diluted for the AgNP with 0.2 mg L^{-1} cysteine and Na_2S, respectively, than for the PVP-AgNP dispersed in natural water, and approximately 20.72 and 7.86 times more diluted, respectively,

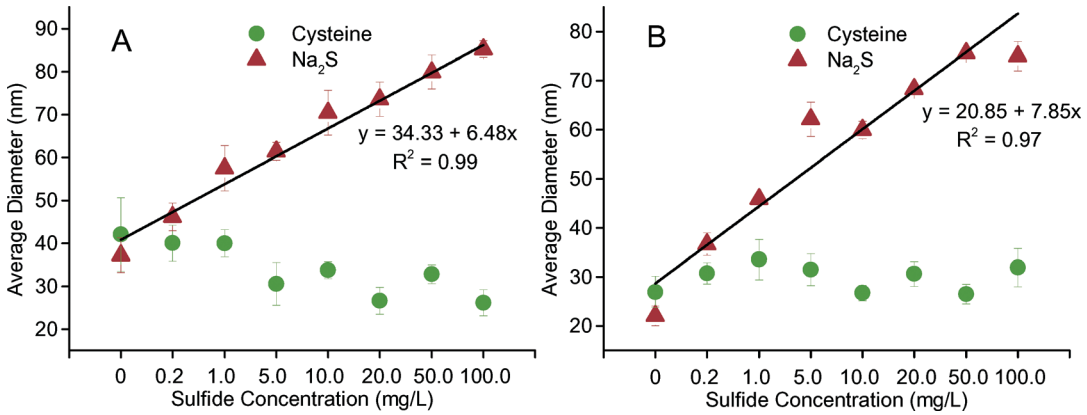

Fig. 2 Average particle size variation of PVP-AgNP (A) and Cit-AgNP (B) after adding various concentrations of cysteine and Na_2S. Both AgNP concentrations were 2 mg L^{-1}. The size was linear fitted to the concentration of Na_2S at 95% confidence intervals.

than the Cit-AgNP in natural water. The specific Ag^+ concentrations were 2.76 ± 0.17 μg L^{-1} and 0.25 ± 0.12 μg L^{-1} for PVP-AgNP treated with 0.2 mg L^{-1} cysteine and Na_2S, respectively, and 0.42 ± 0.15 μg L^{-1} and 1.17 ± 0.15 μg L^{-1}, respectively, for Cit-AgNP at a negligible level. With an increase in sulfide concentration, Ag^+ was diluted further. This is consistent with reports that AgNP dissolution is dependent on sulfidation ratios (S/Ag) and the dissolution rate decreases until Ag^+ could not be detected as the S/Ag ratio increases.[38] In addition, the results indicate that cysteine and Na_2S have the same impact on the dissolution of AgNP with different coatings. Based on these conclusions, in combination with the size variation trends described earlier, it was decided that sulfide concentrations of 1.0 and 50.0 mg L^{-1} would be used for the next tests to distinguish particle sizes using a model.

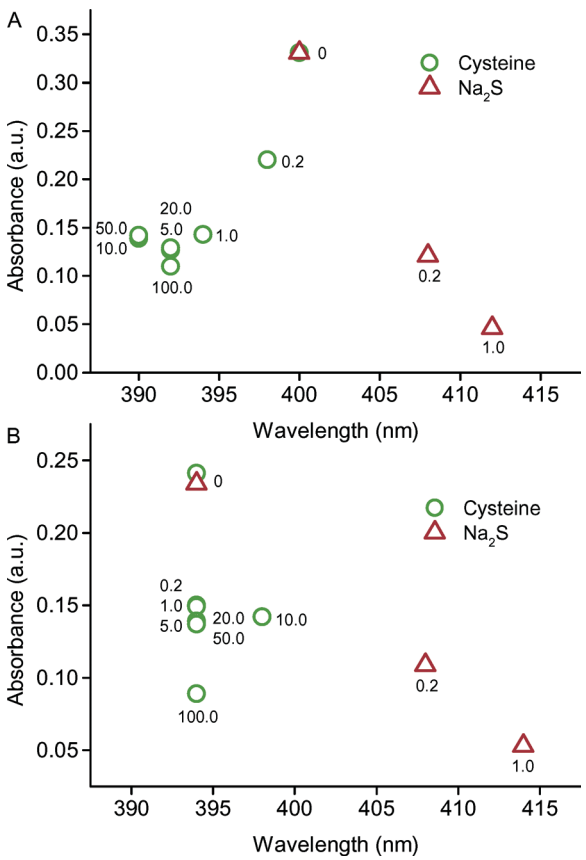

Fig. 3 Changes in the localized surface plasmon resonance (LSPR) absorbance peak of PVP-AgNP (A) and Cit-AgNP (B) after addition of variable concentrations of cysteine and Na_2S for 2 h. Both AgNP concentrations were 2 mg L^{-1}. Parts of the plots after addition of Na_2S were not shown due to strong absorbance masking, in which the absorbance peaks were not obvious.

3.3. Effect of sulfide on the filtration efficiency of AgNP by biofilm

Changes in the sizes of AgNP are vital factors for penetrating a biofilm cell's extracellular polymeric substance (EPS) layer. In the study of Wirth *et al.*, EPS hindered the penetration of low stability AgNP into the biofilms due to aggregated AgNP in the surroundings. By comparison, high stability AgNP may be able to diffuse into the biofilm matrix and gain closer access to the cells.[20] In a biofilm system, the EPS with different chemical properties, such as surface potential and chemical group types, is the substance in direct contact with the AgNP. EPS played a major part in pollutant (including AgNP) adsorption in biofilters. Hence, sulfide-promoted size variation may cause changes in the stability and transfer of AgNP in biofilms, and enhance the treatment efficiency of biofilm systems.

To simulate the practical application, treated natural water was used in the whole assay. The samples were collected from different biofilm layers (*i.e.* 0–0.2, 0.2–0.6, 0.6–1.0, 1.0–1.4, 1.4–1.8, and 1.8–2.0 cm of the biofilm from the surface to the bottom were regarded as different layers for the determination of specific impacts of biofilm depth on AgNP filtration efficiency) and analyzed. Because the released Ag^+ is negligible (ESI,† Fig. S6), the majority of measured AgNP were in their sulfidated form. Fig. 4 shows the percentage of retained AgNP in the different biofilm layers after filtration with 2 mg L^{-1} AgNP in the presence of cysteine or Na_2S. One-way

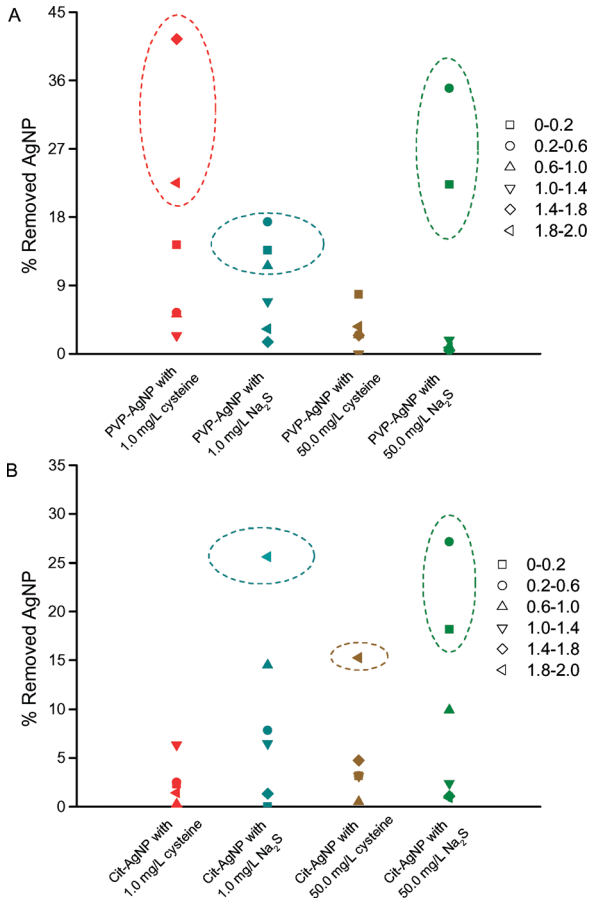

Fig. 4 Percentage of PVP-AgNP (A) and Cit-AgNP (B) in the different biofilm layers. The distinguishable high reservation layers are indicated by dashed circles. All plotted data were the average of at least three independent experiments.

ANOVA indicates the statistical difference between the retained AgNP amounts and the biofilm layer, which is primarily size-oriented in terms of the layer depth with obvious AgNP retention. The majority of PVP-AgNP (Fig. 4A) were retained in the surface layer of the biofilm after reaction with 1.0 mg L^{-1} (13.68% for 0–0.2 cm, 17.34% for 0.2–0.6 cm, and 11.55% for 0.6–1.0 cm) and 50.0 mg L^{-1} (22.27% for 0–0.2 cm and 35% for 0.2–0.6 cm) Na_2S. This is consistent with the increase in size of AgNP that Na_2S promoted, resulting in blockage at the surface layer. The distinguishing retention of AgNP in any layer did not occur at 50.0 mg L^{-1} cysteine. Notably, 1.0 mg L^{-1} cysteine caused a relatively higher retention in the bottom layer of approximately 41.45% for 0–0.2 cm and 22.5% for 0.2–0.6 cm. This is an interesting phenomenon, which can be attributed to the higher penetration of stable AgNP into the EPS as reported by Wirth *et al.*[20] Colloidally stable AgNP suspensions exhibited greater penetration into the EPS and were easily retained in the layers. In combination with an initially larger particle size, the AgNP tended to stay in the bottom layer. By comparison, 50.0 mg L^{-1} cysteine induced greater size reduction of PVP-AgNP than did 1.0 mg L^{-1} cysteine (Fig. 2). Hence, 50.0 mg L^{-1} cysteine induced the smaller size of PVP-AgNP, which outflowed with effluent in major of its content.

Cysteine-treated Cit-AgNP were more stable and could pass through the biofilm smoothly, except for slight blocking (15.26%) from the 1.8–2.0 cm layer in 50.0 mg L^{-1} cysteine. A similar trend was observed for the 50.0 mg L^{-1} Na_2S-treated Cit-AgNP. A differential phenomenon had 1.0 mg L^{-1} Na_2S causing most of the Cit-AgNP to be deposited at 1.8–2.0 cm in a content of 25.64% of the total amount of AgNP. The average size of the Cit-AgNP in the presence of 1.0 mg L^{-1} Na_2S was 45.9 ± 1.0 nm (Fig. 2), which is close to the size of the 1.0 mg L^{-1} cysteine-treated PVP-AgNP (39.9 ± 3.2 nm). This result further indicates the size-oriented AgNP retention.

Fig. 5 shows the removal efficiency for 2 mg L^{-1} AgNP of the biofilm. As for the efficiency of the final treatment, the efficiency of Na_2S treatment of AgNP (both PVP-AgNP and Cit-AgNP) was higher than that of cysteine treatment except for 1 mg L^{-1} sulfide. The final retained AgNP were approximately 3.37 times higher for the PVP-AgNP with 50.0 mg L^{-1} Na_2S than with 50.0 mg L^{-1} cysteine, and approximately 4.21 and 1.99 times higher in terms of Cit-AgNP with 1.0 and 50.0 mg L^{-1} Na_2S, respectively, than with cysteine. The distinguishing higher removal efficiency of 1.0 mg L^{-1} cysteine-treated PVP-AgNP has been explained by the combination of higher penetration and larger particle size. Therefore, inorganic sulfides can improve the retention efficiency of AgNP in biofilm water treatment systems (the maximum retention of AgNP by each biofilm layer was lower than 2%, which is negligible for the whole removal ratio, Fig. S7 in the ESI†). This provides information to help wastewater treatment plants improve their effluent quality (such as removal of potential AgNP) in a new direction.

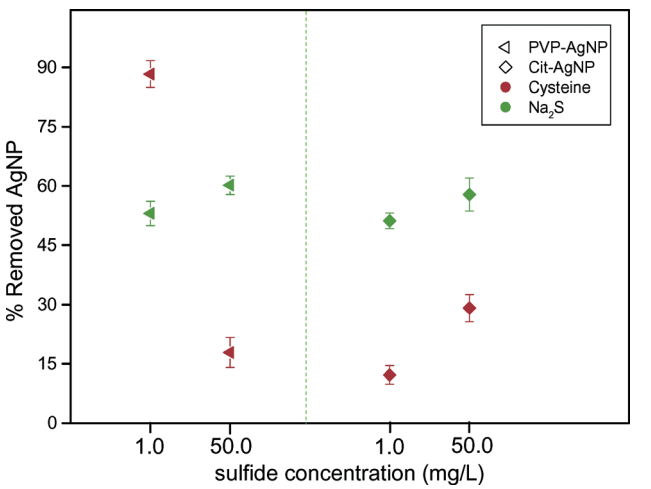

Fig. 5 Whole filtration efficiency of PVP-AgNP and Cit-AgNP after adding 1.0 and 50.0 mg L^{-1} cysteine and Na_2S. Both AgNP concentrations were 2 mg L^{-1}. The error bars represent 95% confidence intervals.

3.4. Effect of sulfide on the toxicity of AgNP to the biofilm

Particle-specific toxicity *versus* Ag^+ toxicity has long been debated in regard to the toxicity to microbes of AgNP. Some studies have suggested that Ag^+ is the main toxic agent, with AgNPs serving mainly as a source of Ag^+.[39,40] Other studies have shown a distinct role of the nanoparticles themselves through AgNP suspension toxicity, although the particle-specific toxicity mechanism remains unclear.[41,42] Here, we indicate that "particle-specific" toxicity plays a prominent role but without distinguishing the role of dissolved silver introduced alone, *i.e.*, the effect on the biofilm was not evident when dissolved silver was added, but AgNPs may enter cells and deliver a high localized Ag^+ flux that impairs the cells. The special biochemical toxicity mechanism was the same, but the particle plays a major role in the toxicity process.

Fig. 6 shows that a PVP-AgNP solution with 1.0 mg L^{-1} cysteine exhibits viability loss in the biofilm layer at 1.8–2.0 cm ($p < 0.001$) and there is no significant difference when the cysteine concentration increases to 50.0 mg L^{-1} (cysteine has no effect on the biofilm viability as shown in Fig. S8 of the ESI†). The toxicity of nanoparticles depends on their size,[43] because a higher cysteine concentration induced the toxicity of smaller-sized AgNP that were discharged into the effluent. In terms of Na_2S, a slightly different viability loss ($p < 0.05$) at 0 cm (surface) was observed for 1.0 mg L^{-1} and the difference became more distinguishing ($p < 0.01$) at 0 cm and 0.2 cm for 50.0 mg L^{-1}. This is consistent with the deposition of AgNP at the upper layer (Fig. 4A). Cysteine decreased the biofilm viability in contrast to Na_2S, which indicates that Na_2S-promoted aggregation can decrease the toxicity of AgNP. In other words, sulfidation of PVP-AgNP cannot restrain its particle-specific toxicity as long as it is a monodispersed particle, because sulfidation will reduce Ag^+ release to a negligible level. This conclusion verifies the results of Yin *et al.* that showed that cysteine (which binds Ag^+) mitigated the effects of $AgNO_3$ but did not reduce the toxicity of AgNP treatments.[44] In addition, a distinguishing level of biofilm viability loss occurred at 0–0.4 cm and 1.6–2.0 cm. Hence, we divided the biofilm into three levels, *i.e.* the upper level 0–0.4 cm, the middle level 0.4–1.6 cm, and the bottom level 1.6–2.0 cm.

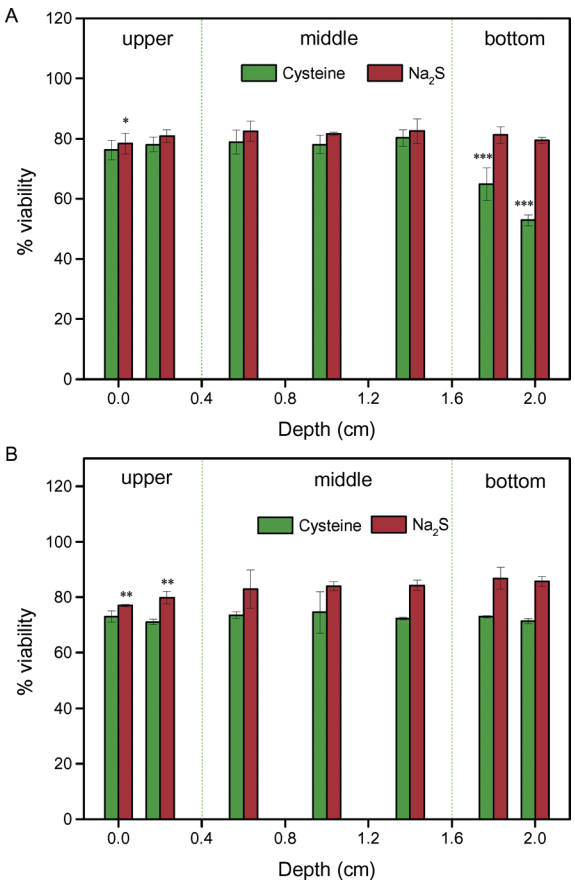

Fig. 6 PVP-AgNP induced viability change in the *P. chrysosporium* biofilm in the presence of 1.0 mg L^{-1} sulfide (A) and 50.0 mg L^{-1} sulfide (B). The viability of the blank sample was set as 100%. The viability of treated samples was a relative value in comparison with the blank. '*' denotes $p < 0.05$; '**' denotes $p < 0.01$; and '***' denotes $p < 0.001$ as compared to the viability of each depth; any significant difference was determined by one-way ANOVA.

For Cit-AgNP (Fig. S9 of the ESI†), 50.0 mg L^{-1} cysteine induced distinguishing viability loss in the bottom layer (1.8 cm, $p < 0.01$ and 2.0 cm, $p < 0.001$), which was also the site of AgNP accumulation, but there was no significant difference when the cysteine concentration was 1.0 mg L^{-1}. Na_2S promoted a slightly different viability loss in the bottom layer (2.0 cm, $p < 0.05$) for 1.0 mg L^{-1} and in the upper layer (0 cm and 0.2 cm, $p < 0.05$) for 50.0 mg L^{-1}. A similar decrease in biofilm viability loss in the presence of cysteine was observed in contrast to Na_2S. For the two types of AgNP, cysteine treatment induced larger viability loss, especially in the AgNP accumulation sites, indicating the prominent role of particle-specific toxicity.

To demonstrate the particle-specific effect, 2 mg L^{-1} $AgNO_3$ was added to the sulfide to perform the toxicity assay (Fig. S10 of the ESI†). Our results show that sulfide, especially at higher concentrations, can effectively quench the phytotoxicity of $AgNO_3$. Thus, the toxicity of AgNP was clearly related to specific particles introduced to these systems. AgNP can provoke the biotic production of reactive oxygen species (ROS),[45] and the resulting oxidative stress can be a mediator of cell apoptosis.[46] Regarding inhibition of Ag^+ release, both cysteine and Na_2S addition decreased the cellular production of intracellular ROS when compared to pure AgNP (the percentage values are approximately 75.2% and 69.0% for 1.0 mg L^{-1} cysteine and Na_2S-treated PVP-AgNP, respectively, and approximately 51.1% and 27.8% for 50.0 mg L^{-1} cysteine and Na_2S-treated PVP-AgNP, respectively; Fig. S11A of the ESI†). Similar results were observed in Cit-AgNP, as shown in Fig. S11B of the ESI.† Although Ag^+ release was inhibited by both sulfides, the ROS produced by cysteine treatment is obviously higher compared with Na_2S treated groups. The distinguishing ROS production demonstrates that cysteine cannot reduce the toxicity of AgNP associated with their particle-specific toxicity. However, we did not deny the

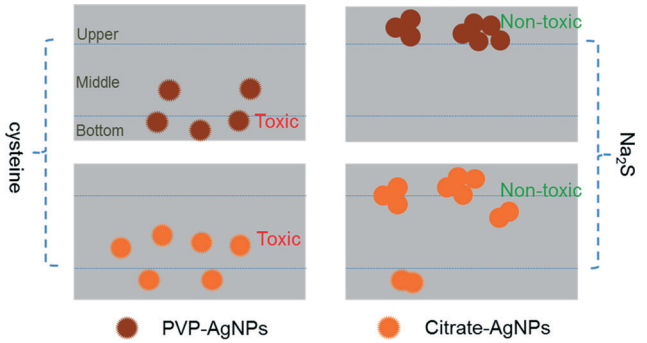

Fig. 7 Schematic of AgNP retention in biofilm layers.

possibility that access to the cell and a high localized Ag^+ flux to the cell could produce these results.[20,47] The specific biochemical toxicity mechanism may be the same, but the AgNP play a prominent role in the procedures.

3.5. Environmental implication

The organic sulfide, cysteine, and the inorganic sulfide, Na_2S, exhibited different effects on the fate of AgNP in the *P. chrysosporium* biofilm (Fig. 7). Due to aggregation that occurred in the presence of Na_2S, AgNP in a Na_2S-abundant region tended to deposit on the upper layer of the biofilm. In contrast, cysteine stabilized the AgNP in the solution, causing AgNP to be discharged into the effluent or mostly deposited on the bottom of the biofim. Hence, it is important to exploit this specific effect due to the fact that various sulfides exist in wastewater and *P. chrysosporium* is used extensively in biological wastewater treatment systems. This study illustrates the specific transfer of AgNP into each biofilm layer and the final removal efficiency in the presence of cysteine or Na_2S. It provides useful information to those using biofilms in the wastewater treatment field.

The loss of bioavailable free silver as a result of sulfidation decreased the overall acute biofilm toxicity,[48,49] but different sulfide sources had inequable influence on the toxicity of AgNP to biofilms. For cysteine, silver ion toxicity toward biofilms was mitigated while particle-specific toxicity was maintained for colloidally stable AgNP. Na_2S seems to eliminate the particle-specific toxicity due to aggregation. Therefore, environmental sulfide may simultaneously affect the activity of biofilm cells, in turn, producing distinguished processing capacity of wastewater.

4. Conclusions

In summary, we investigated the distribution of PVP-AgNP and Cit-AgNP in a *P. chrysosporium* biofilm microcosm, with either cysteine, or Na_2S, present in the test environment. Both types of AgNP tested easily penetrated the *P. chrysosporium* biofilm and remained mostly in the bottom layer (1.6–2.0 cm) when cysteine was present. In contrast, both types of AgNP remained in the surface layer (0–0.4 cm) in an aggregated form in the presence of Na_2S. An obvious particle-specific toxicity to the film was observed in cysteine-abundant surroundings. In the presence of Na_2S, the toxicity of both types of AgNP was completely inhibited. This work indicates that sulfide-induced particle stability was crucial to AgNP transfer and toxicity in biofilms.

Acknowledgements

This study was financially supported by the National Natural Science Foundation of China (51579099, 51521006, 51479072 and 51408209), the Program for Changjiang Scholars and Innovative Research Team in University (IRT-13R17), and the Hunan Provincial Innovation Foundation for Postgraduate (CX2016B134).

References

1 Z. Sheng and Y. Liu, *Water Res.*, 2011, **45**, 6039–6050.
2 S. J. Klaine, P. J. Alvarez, G. E. Batley, T. F. Fernandes, R. D. Handy, D. Y. Lyon, S. Mahendra, M. J. McLaughlin and J. R. Lead, *Environ. Toxicol. Chem.*, 2008, **27**, 1825–1851.
3 A. M. El Badawy, K. G. Scheckel, M. Suidan and T. Tolaymat, *Sci. Total Environ.*, 2012, **429**, 325–331.
4 C. Levard, E. M. Hotze, G. V. Lowry and G. E. Brown, *Environ. Sci. Technol.*, 2012, **46**, 6900–6914.
5 C. Zhang, Z. Hu and B. Deng, *Water Res.*, 2016, **88**, 403–427.
6 R. Kaegi, A. Voegelin, C. Ort, B. Sinnet, B. Thalmann, J. Krismer, H. Hagendorfer, M. Elumelu and E. Mueller, *Water Res.*, 2013, **47**, 3866–3877.
7 W. J. Stark, *Angew. Chem., Int. Ed.*, 2011, **50**, 1242–1258.
8 L. Li, H. Wu, W. J. G. M. Peijnenburg and C. A. M. van Gestel, *Nanotoxicology*, 2015, **9**, 792–801.
9 H. Zhang, J. A. Smith and V. Oyanedel-Craver, *Water Res.*, 2012, **46**, 691–699.
10 K. A. Huynh and K. L. Chen, *Environ. Sci. Technol.*, 2011, **45**, 5564–5571.
11 W. Zhang, J. Crittenden, K. Li and Y. Chen, *Environ. Sci. Technol.*, 2012, **46**, 7054–7062.
12 N. Akaighe, R. Maccuspie, D. A. Navarro, D. S. Aga, S. Banerjee, M. Sohn and V. K. Sharma, *Environ. Sci. Technol.*, 2011, **45**, 3895–3901.
13 S. J. Yu, Y. G. Yin, J. B. Chao, M. H. Shen and J. F. Liu, *Environ. Sci. Technol.*, 2014, **48**, 403–411.
14 K. Savolainen, H. Alenius, H. Norppa, L. Pylkkänen, T. Tuomi and G. Kasper, *Toxicology*, 2010, **269**, 92–104.
15 J. Fabrega, S. N. Luoma, C. R. Tyler, T. S. Galloway and J. R. Lead, *Environ. Int.*, 2011, **37**, 517–531.
16 F. Piccapietra, L. Sigg and R. Behra, *Environ. Sci. Technol.*, 2012, **46**, 818–825.
17 A. R. Bielefeldt, M. W. Stewart, E. Mansfield, R. S. Summers and J. N. Ryan, *Water Res.*, 2013, **47**, 4032–4039.
18 J. Liu, S. Legros, F. Von der Kammer and T. Hofmann, *Environ. Sci. Technol.*, 2013, **47**, 4113–4120.
19 G. Brunetti, E. Donner, G. Laera, R. Sekine, K. G. Scheckel, M. Khaksar, K. Vasilev, G. D. Mastro and E. Lombi, *Water Res.*, 2015, **77**, 72–84.

20 S. M. Wirth, G. V. Lowry and R. D. Tilton, *Environ. Sci. Technol.*, 2012, **46**, 12687–12696.

21 Z. M. Xiu, J. Ma and P. J. Alvarez, *Environ. Sci. Technol.*, 2011, **45**, 9003–9008.

22 Y. Yang, B. Renata, S. Laura, F. F. Paloma, P. Smitha and S. Kristin, *Nanotoxicology*, 2015, **9**, 54–63.

23 W. Stumm and J. J. Morgan, *Aquatic chemistry: chemical equilibria and rates in natural waters*, Third edn, A Wiley-Interscience Publication, 1996.

24 D. L. Huang, G. M. Zeng, C. L. Feng, S. Hu, M. H. Zhao, C. Lai, Y. Zhang, X. Y. Jiang and H. L. Liu, *Chemosphere*, 2010, **81**, 1091–1097.

25 Z. Huang, G. Chen, G. Zeng, A. Chen, Y. Zuo, Z. Guo, Q. Tan, Z. Song and Q. Niu, *J. Hazard. Mater.*, 2015, **289**, 174–183.

26 A. Chen, G. Zeng, G. Chen, C. Zhang, M. Yan, C. Shang, X. Hu, L. Lu, M. Chen, Z. Guo and Y. Zuo, *Chemosphere*, 2014, **109**, 208–212.

27 S. D. Solomon, M. Bahadory, A. V. Jeyarajasingam, S. A. Rutkowsky, C. Boritz and L. Mulfinger, *J. Chem. Educ.*, 2007, **84**, 322–325.

28 J. Liu and R. H. Hurt, *Environ. Sci. Technol.*, 2010, **44**, 2169–2175.

29 L. Deng, X. Y. Ouyang, J. Y. Jin, C. Ma, Y. Jiang, J. Zheng, J. S. Li, Y. H. Li, W. H. Tan and R. H. Yang, *Anal. Chem.*, 2013, **85**, 8594–8600.

30 T. K. Kirk, E. Schultz, W. J. Connors, L. F. Lorenz and J. G. Zeikus, *Arch. Microbiol.*, 1978, **117**, 277–285.

31 Y. H. Luo, S. B. Wu, Y. H. Wei, Y. C. Chen, M. H. Tsai, C. C. Ho, S. Y. Lin, C. S. Yang and P. Lin, *Chem. Res. Toxicol.*, 2013, **26**, 662–673.

32 A. Chen, G. Zeng, G. Chen, L. Liu, C. Shang, X. Hu, L. Lu, M. Chen, Y. Zhou and Q. Zhang, *Process Biochem.*, 2014, **49**, 589–598.

33 S. L. Loo, W. B. Krantz, A. G. Fane, Y. Gao, T. T. Lim and X. Hu, *Environ. Sci. Technol.*, 2015, **49**, 2310–2318.

34 Z. Guo, G. Chen, G. Zeng, Z. Li, A. Chen, M. Yan, L. Liu and D. Huang, *RSC Adv.*, 2014, **4**, 59275–59283.

35 L. R. Pokhrel, B. Dubey and P. R. Scheuerman, *Environ. Sci. Technol.*, 2013, **47**, 12877–12885.

36 A. P. Gondikas, A. Morris, B. C. Reinsch, S. M. Marinakos, G. V. Lowry and H. K. Heileen, *Environ. Sci. Technol.*, 2012, **46**, 7037–7045.

37 H. Liu, Y. Ye, J. Chen, D. Lin, Z. Jiang, Z. Liu, B. Sun, L. Yang and J. Liu, *Chem. – Eur. J.*, 2012, **18**, 8037–8041.

38 C. Levard, B. C. Reinsch, F. M. Michel, C. Oumahi, G. V. Lowry and G. E. Brown Jr., *Environ. Sci. Technol.*, 2011, **45**, 5260–5266.

39 A. J. Miao, K. A. Schweh, C. Xu, S. J. Zhang, Z. P. Luo, A. Quigg and P. H. Santschi, *Environ. Pollut.*, 2009, **157**, 3034–3041.

40 S. Kim, J. E. Choi, J. Choi, K. H. Chung, K. Park, J. Yi and D. Y. Ryu, *Toxicol. In Vitro*, 2009, **23**, 1076–1084.

41 G. A. Sotiriou and S. E. Pratsinis, *Environ. Sci. Technol.*, 2010, **44**, 5649–5654.

42 J. Fabrega, S. R. Fawcett, J. C. Renshaw and J. R. Lead, *Environ. Sci. Technol.*, 2009, **43**, 7285–7290.

43 M. Auffan, J. Rose, J. Y. Bottero, G. V. Lowry, J. P. Jolivet and M. R. Wiesner, *Nat. Nanotechnol.*, 2009, **4**, 634–641.

44 L. Yin, Y. Cheng, B. Espinasse, B. P. Colman, M. Auffan, M. Wiesner, J. Rose, J. Liu and E. S. Bernhardt, *Environ. Sci. Technol.*, 2011, **45**, 2360–2367.

45 O. Choi and Z. Q. Hu, *Environ. Sci. Technol.*, 2008, **42**, 4583–4588.

46 Y. H. Hsin, C. F. Chen, S. Huang, T. S. Shih, P. S. Lai and P. J. Chueh, *Toxicol. Lett.*, 2008, **179**, 130–139.

47 I. L. Hsiao, Y. K. Hsieh, C. F. Wang, I. C. Chen and Y. J. Huang, *Environ. Sci. Technol.*, 2015, **49**, 3813–3821.

48 B. C. Reinsch, C. Levard, Z. Li, R. Ma, A. Wise, K. B. Gregory, G. E. Brown Jr. and G. V. Lowry, *Environ. Sci. Technol.*, 2012, **46**, 6992–7000.

49 C. Levard, E. M. Hotze, B. P. Colman, A. L. Dale, L. Truong, X. Y. Yang, A. J. Bone, G. E. Brown Jr., R. L. Tanguay, R. T. Di Giulio, E. S. Bernhardt, J. N. Meyer, M. R. Wiesner and G. V. Lowry, *Environ. Sci. Technol.*, 2013, **47**, 13440–13448.